

See discussions, stats, and author profiles for this publication at: <https://www.researchgate.net/publication/332968221>

Fusion of Underwater Image Enhancement and Restoration

Article in International Journal of Pattern Recognition and Artificial Intelligence · July 2019

DOI: 10.1142/S0218001420540075

CITATIONS
34

READS
1,818

2 authors:



Rajni Sethi

7 PUBLICATIONS 91 CITATIONS

[SEE PROFILE](#)



Indu Sreedevi

Delhi Technological University

208 PUBLICATIONS 1,817 CITATIONS

[SEE PROFILE](#)

International Journal of Pattern Recognition and Artificial Intelligence
© World Scientific Publishing Company

Fusion of Underwater Image Enhancement and Restoration

Rajni Sethi

*Department of Information Technology,
Delhi Technological University, Delhi
rajni_gumber23@yahoo.com*

S.Indu

*Department of Electronics and Communication Engineering,
Delhi Technological University, Delhi
rajni_gumber23@yahoo.com*

Optical properties of water distort the quality of underwater images. Underwater images are characterized by poor contrast, color cast, noise and haze. These images need to be pre-processed so as to get some information. In this paper, a novel technique named Fusion of Underwater Image Enhancement and Restoration (FUIER) has been proposed which enhances as well as restores underwater images with a target to act on all major issues in underwater images, i.e., color cast removal, contrast enhancement and dehazing. It generates two versions of the single input image and these two versions are fused using Laplacian pyramid based fusion to get the enhanced image. The proposed method works efficiently for all types of underwater images captured in different conditions (turbidity, depth, salinity etc.). Results obtained using the proposed method are better than those for state-of-the-art methods.

Keywords: Underwater images; image enhancement; image restoration; pyramid based fusion; dehazing

1. Introduction

A major portion of the Earth is covered by water and life in these water bodies forms a significant part of the ecosystem. Therefore, study of the aquatic environment is gaining a lot of attention for which various videos and images are captured to acquire information. Underwater imagery not only unravels the mystery beneath water but also provides information required for underwater scientific studies, such as understanding marine ecology ³⁸, assisting aquatic robots ³⁴, understanding underwater geology ⁴⁴ and fish species recognition ³⁰. Underwater videos and images are of poor quality due to the optical properties of water. The physical property of water to absorb the longest wavelengths first, leads to the dominance of red color and domination of green and blue color in underwater images. The scattering property of water leads to low visibility even in clear water and almost negligible visibility in turbid water. Thus, Underwater images are of very poor quality with limited range of visibility, poor contrast, noise and a greenish blue color cast ³¹. Artificial light is

2 *Rajni Sethi, S.Indu*

utilized to tackle poor visibility and color loss, but it leads to non-uniform lighting. Owing to these problems, there is need for pre-processing of underwater images so as to use them for various studies.

In this paper, a novel underwater image processing technique has been proposed which is computationally inexpensive and targets all the major issues in underwater images. The proposed methodology is named as Fusion of Underwater Image Enhancement and Restoration (FUIER). For image enhancement, Histogram Equalization (HE) ¹⁶, a well known basic color correction technique, has been applied on three color channels of RGB image for generating the first version of the input image. Now, the second version is created by the contrast stretching of three channels of the input RGB image over the whole dynamic range followed by dehazing based on dark channel prior ¹⁸. Now, these two versions are fused using weighted laplacian pyramid decomposition based fusion. Results of FUIER are promising and better as compared to state-of-the-art techniques.

The article is composed in following sections. Section 2 gives an insight into related work on underwater image processing and the motivation behind FUIER. Section 3 presents its working. Section 4 compares FUIER with state-of-the-art methods and finally, section 5 concludes the article and discusses the future scope of the proposed technique.

2. Literature Review

A lot of work is being done in the field of underwater image processing in directions of both image enhancement and image restoration. Image enhancement methods give researchers the liberty to experiment with images so that a pleasant image can be obtained using different spatial or frequency domain filters. One of the popular and traditional method for enhancement is histogram equalization (HE) ¹⁶ which distributes the intensities of all the color channels over the entire dynamic range. HE tends to change the balance of RGB images leading to artifacts. But it has applicability for underwater images as the three color channels are already unevenly distributed in this case but artifacts are still present in the resultant image. Adaptive HE ³³ processes the image by dividing it into parts and then applying HE. It increases the complexity over HE but can address the problem of non-uniform contrast in underwater images. However, color distortion problem is still unaddressed. ICM (Integrated Colour Model) ²⁰ and UCM (Unsupervised Color correction Method) ¹⁹ are techniques employing contrast stretching in different color formats to obtain visually appealing results. In ⁵, a pre-processing step using various filters has been proposed to enhance the image quality by removing noise. Lu *et al.* ²⁷ used trigonometric filter for enhancement of underwater images. Gao *et al.* ¹⁴ devised a new mathematical model called fractional directional derivative for contrast enhancement of images. Wang *et al.* ³⁶ formulated a smooth rank function for low rank matrix which can remove a combination of noises like gaussian, salt and pepper etc. from the images. These techniques have their own advantage of

being computationally easy and not requiring any knowledge of image formation. A disadvantage of these techniques is that they overstretch the histogram and sometime introduce artifacts (false color, artificial appearance) in the image.

Image restoration methods employ the knowledge of the image formation model to restore the original scene from the captured scene. These methods rely on finding or estimating parameters of the equation of underwater image formation²¹ shown in Eq. 1.

$$I(x, y) = J(x, y)e^{-\eta \cdot d(x, y)} + B(x, y) \cdot (1 - e^{-\eta \cdot d(x, y)}) \quad (1)$$

where, $I(x, y)$ is captured image, $J(x, y)$ is the original image, $d(x, y)$ denotes distance of the object from the camera, η represents attenuation coefficient of medium and $B(x, y)$ represents the background light. $e^{-\eta \cdot d(x, y)}$ represents the transmission map. Thus, the aim of image restoration techniques is to find $J(x, y)$ from $I(x, y)$. This given equation of underwater image formation is similar to the equation of light propagation with additional factors affecting the attenuation coefficient (scattering and absorption). In recent years, dehazing using dark channel prior¹⁸ has gained a lot of attention owing to its effective results in removing the haze from images captured in atmospheric medium. Thus, a lot of research has been focused on applying dehazing algorithms based on different priors on the underwater images. For instance, Chao *et al.*¹⁰ and Carlevaris-Bianco *et al.*⁸ used dark channel prior to clarify blurred underwater images but failed to color correct the images. Yang *et al.*⁴² employed dark channel prior for image deblurring followed by a color correction method. Chaing *et al.*¹¹ proposed a dark channel prior based algorithm which further removes artifacts caused by artificial light. Jolla *et al.*²³ developed a dark channel prior based algorithm in which estimation of dark channel is done using image blurriness model. Gao *et al.*¹⁵ modified the dark channel prior to bright channel prior for enhancing underwater images. Galdran *et al.*¹³ formulated the problem around red channel restoration as red color attenuates the most in the underwater environment. Li *et al.*²⁶ proposed an algorithm which used minimum information loss principle for image dehazing followed by a contrast enhancement algorithm for further enhancement of the image. The main focus of these underwater image dehazing algorithms is the removal of the hazy appearance of underwater images, but the other issues remain unattended. Some research works have tried to incorporate color correction or contrast correction along with dehazing but the results are not satisfactory and moreover, the methods are computationally expensive and require estimation of various parameters. Since dehazing based techniques rely on parameter tuning, some researchers are also focusing on training convolutional neural network (CNN) with image restoration techniques to dehaze underwater images^{29, 37}. Another deep neural network based study for underwater image enhancement³ has trained the CNN for finding the parameters of image formation model using synthetic underwater images. Trained neural networks give good results. However, it requires a lot of time to exhaustively train the neural networks with every type of underwater image to get effective results.

4 *Rajni Sethi, S.Indu*

Some researchers have worked on underwater images using a fusion of multiple versions of the input image by using different enhancement methods and then tried to incorporate features required for an enhanced image from all the versions using weight maps. These methods give better results than applying those different techniques in any specific order as weight maps dictate the importance of one technique over another. Multi-scale representation of features helps in enhancing the performance of algorithms and can be used by vector-based feature extraction and classification algorithms³⁹. Celebi *et al.*⁹ proposed Empirical Mode Decomposition (EMD) of three spectral components to generate intrinsic mode functions and then employed weight maps to fuse these intrinsic mode functions. But this technique requires parameter tuning to find the residual function of EMD. Ancuti *et al.*² proposed a fusion of two versions (color corrected and contrast corrected) of input image using four different weight maps derived from those versions. In¹, Ancuti *et al.* extended² by modifying the contrast correction method and reducing the number of weight maps. Both the techniques employ multi-scale Laplacian pyramid decomposition based fusion and give good results but a little haze is still present in the output. Zhang *et al.*⁴⁵ proposed an underwater image enhancement method which first restores the image and then fuses the two versions of the restored image using multi-scale fusion but the results are not better than those obtained by Ancuti *et al.*¹.

2.1. Motivation Behind FUIER

From the literature, it is clear that there is a plethora of work presented in the literature which either performs intensity manipulation using spatial domain filters or tries to restore the original image from captured image using the image formation model. Some of them apply image restoration technique followed by image enhancement. In this way, they try to remove all the problems in underwater images, but the result has disadvantages of both, i.e., increased computational complexity and artifacts in the output image. As we know both types of techniques have their advantages and disadvantages, the motivation behind this work is to develop an algorithm which tackles all the major problems in underwater images and is computationally less intensive. FUIER combines the color and contrast correction ability of image enhancement based methods and haze removal property of image restoration based methods. Furthermore, image restoration technique is chosen in a way that computation and time complexity of the overall algorithm is low and artifacts of image enhancement methods can be avoided. Multi-scale weighted Laplacian pyramid based fusion has been employed which ensures that only desired features are taken in the final image.

In FUIER, two versions of the input image are created. the first version is a histogram equalized version of the input image which leads to color correction. The second version is contrast stretched version of the input image followed by dehazing

using dark channel prior based method. Two weight maps, namely local entropy weight map and gradient weight map have been calculated for both the versions. Now, these two versions are fused using multi-scale weighted Laplacian pyramid decomposition⁷ based fusion. These weights control the contribution of each version towards the final enhanced image without introducing artifacts and halos. The main contributions of FUIER are as follows:

- (a) It employs simple and computationally less intensive techniques which produce results possessing the qualities required in underwater images.
- (b) Effective weight maps have been formulated to extract the desired features from the different versions.
- (c) It is an adaptive method which works for every type of underwater image captured at any depth, in any saline or turbid medium.

The next section explains FUIER in detail.

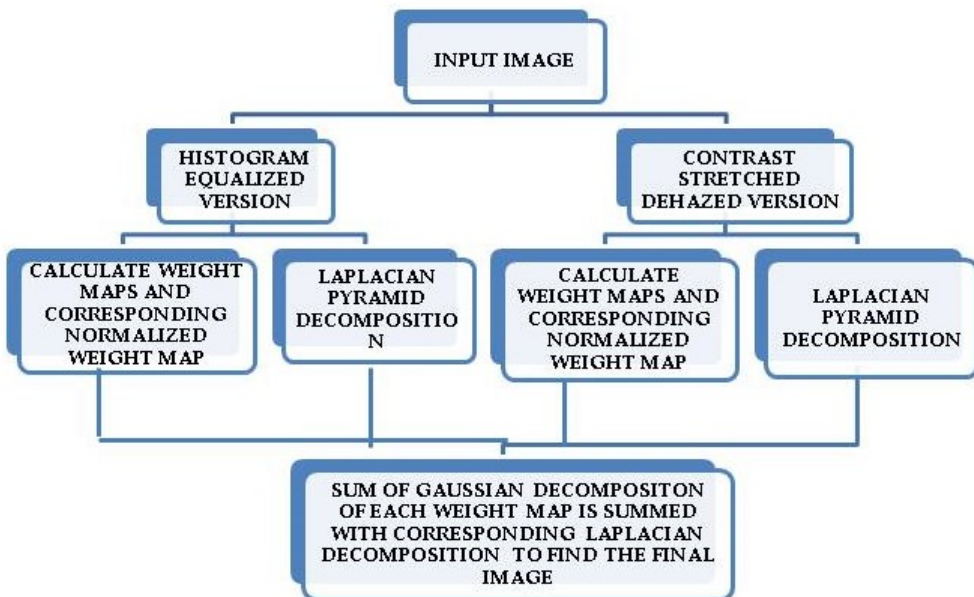


Fig. 1: Work Flow of FUIER

3. Working of FUIER

FUIER employs computationally simple image enhancement and image restoration methods to achieve the aim of removing the problem of color cast (by histogram equalization), poor contrast (by contrast correction) and hazy appearance (by dark channel prior based method). The basic workflow of FUIER is shown in Fig. 1. FUIER works at three levels: deriving two versions of the input image, calculating

weight maps and fusion of the two versions with corresponding weight maps at multiple scales.

3.1. Generation of Two Versions for Fusion

The first version for fusion process is a color corrected version which is generated by a traditional image enhancement method named Histogram Equalization (HE)¹⁶. HE is a simple method to enhance the contrast when applied on a grayscale image but when it is applied on three color channels individually in case of underwater images, it uniformly distributes the intensity value over the whole dynamic range thereby removing the color cast. The reason behind this phenomenon is that it removes the domination of a single color channel in the image by spreading the intensities of all color channels over the dynamic range of intensities which can be seen in Fig. 2. Fig. 2 shows an underwater image and its histogram before and after applying HE.

The second version for the fusion process is a contrast corrected dehazed image. Contrast correction is done by simply stretching the histogram of all the color channels to span the whole dynamic range using Eq. 2.

$$CI_c(x, y) = (I_c(x, y) - \min I_c) * (\text{Max} - \text{Min}) / (\max I_c - \min I_c) \quad (2)$$

where $CI_c \in [r, g, b]$ is the contrast corrected image, $\max I_c$ and $\min I_c$ is the maximum and minimum intensity value respectively of each color channel and Max and Min denotes the maximum and minimum possible intensity value respectively for an image e.g. 255 and 0 are the maximum and minimum possible value for an 8 bit RGB image.

After contrast stretching, dehazing of the image is done by dark channel prior¹⁸. As mentioned earlier, a lot of work has been done in the field of underwater images using either the original dark channel prior or its modified versions, but we have chosen the original dark channel prior because it is a simple yet powerful method for dehazing to remove the haze present in underwater images. For a hazy image, the image is modelled as in Eq. 3.

$$I(x) = J(x)t(x) + A(1 - t(x)) \quad (3)$$

where $I(x)$ is the observed radiance, $J(x)$ is the actual radiance, $t(x)$ is the transmission map and A is the atmospheric light

The above equation is same as Eq. 1, which is the image formation model for underwater images. In this approach, we first find the dark channel using the assumption that the dark channel of a haze-free image is zero which can be defined as shown in Eq. 4.

$$J^{dark}(x) = \min_{c=r, g, b} \left(\min_{y \in \Omega(x)} (J^c(y)) \right) \quad (4)$$

where J^{dark} is the dark channel and Ω is 15X15 neighborhood is chosen for estimating the dark channel.

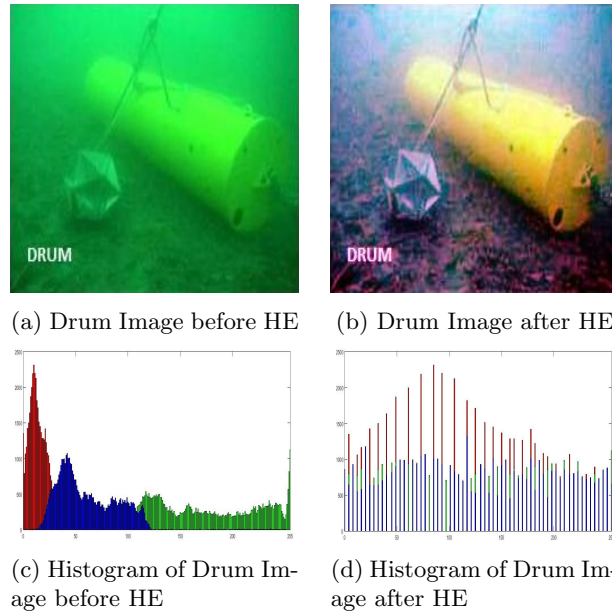


Fig. 2: Drum image and its histogram before and after applying HE

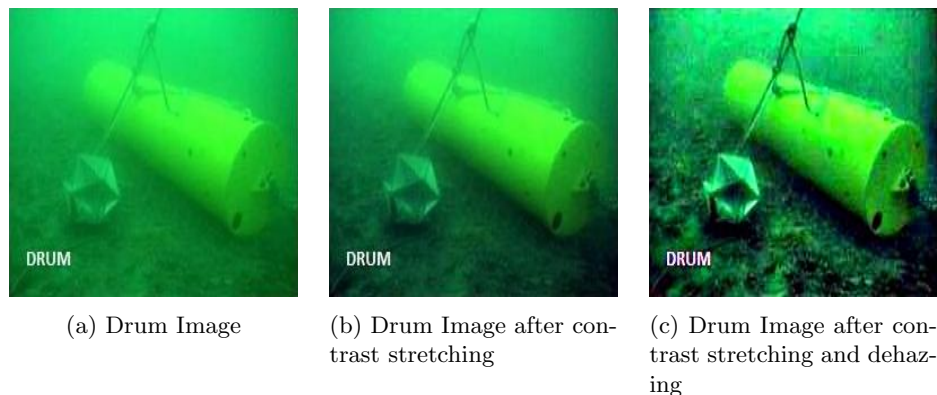


Fig. 3: Drum image after applying contrast stretching and dehazing to obtain the second version for fusion

Firstly, the atmospheric light is estimated by using this dark channel. The top 0.1 % percent of the brightest pixels are chosen from the dark channel and then among these pixels, the highest intensity pixel from the image I is chosen to represent 'A' (atmospheric light). We then compute the raw transmission map $\tilde{t}(x)$ by using Eq.

5.

$$\tilde{t}(x) = 1 - \min_c \left(\min_{y \in \Omega(x)} \frac{I^c(y)}{A} \right) \quad (5)$$

$\min_c \left(\min_{y \in \Omega(x)} \frac{I^c(y)}{A} \right)$ denotes dark channel of the normalized haze image $\frac{I^c(y)}{A}$ which directly provides the estimation of the transmission.

Then, the raw transmission map is refined by using guided filter ¹⁷ to speed up computation instead of soft matting used in ¹⁸. Finally, haze-free image is recovered using Eq. 6 from the refined transmission map ($t(x)$) and estimated atmospheric light (A).

$$J(x) = \frac{(I(x) - A)}{\max(t(x), t_0)} + A \quad (6)$$

t_0 is chosen 0.1 as mentioned in ¹⁸. Fig. 3 shows the contrast stretched and dehazed image version of the drum image.

3.2. Weight Maps for fusion

Two new weight maps are designed in order to incorporate the desired features in the final image. We want the final image to have good contrast along with better information content. Depending on the weight values, a pixel with higher weight is given priority over other to appear in the final enhanced image.

Local Entropy weight map Local entropy gives an estimate of the variation of information in the local regions of the image which reduces the effect of noise. Local Entropy serves as an indicator in many applications like region extraction ⁴¹, saliency descriptor ²⁴ etc.. Local entropy is calculated by first converting RGB image into HSV format and using the MATLAB function 'entropyfilt' with default neighborhood values on the value (V) component of the image denoted by W_V . This weight map estimates only one aspect, i.e., the information content of the image. Thus, we need another weight map for the estimation of contrast of the image for which we have another weight metric.

Gradient weight map Gradient weight map estimates the variance of the color saturation level of an image. Gradient weight map is calculated using directional gradients of the saturation (S) component of the HSV image. Gradient weight map (W_G) is calculated using Eq. 7.

$$\begin{aligned} G_x(x, y) &= S(x - 1, y) - S(x + 1, y) \\ G_y(x, y) &= S(x, y - 1) - S(x, y + 1) \\ W_G(x, y) &= \sqrt{G_x(x, y)^2 + G_y(x, y)^2} \end{aligned} \quad (7)$$

Finally, for each input k, a single weight map (w_k) is derived by summing up the two weight maps. Final normalized weight map (W_k) for each input image k is

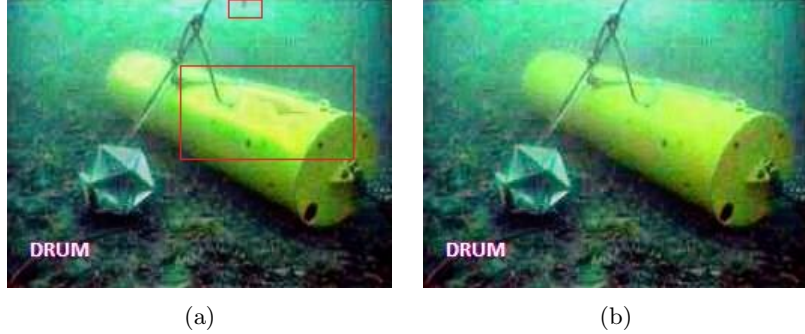


Fig. 4: Enhanced drum image using (a) weighted addition (b) Multi-scale Laplacian pyramid decomposition based fusion

derived using Eq. 8.

$$\begin{aligned} w_k(x, y) &= W_V(x, y) + W_G(x, y) \\ W_k(x, y) &= w_k(x, y) / \left(\sum_{j=1}^2 w_j(x, y) + 0.001 \right) \end{aligned} \quad (8)$$

where, w_j refers to weight maps of the two input images and a constant '0.001' is added to avoid divide by zero error.

3.3. Multi-scale Pyramid decomposition based fusion

Image fusion can be done by simply adding the two versions of the input image using Eq. 9, but such an addition leads to artifacts in the final image. To avoid artifacts, we opt for multi-scale Laplacian pyramid decomposition based fusion ⁷.

$$Final(i, j) = \sum_{k=1}^2 W_k(i, j) I_k(i, j) \quad (9)$$

Fig. 4 shows the result of drum image using simple weighted addition and multi-scale Laplacian pyramid decomposition based fusion. Red boxes in the weighed fusion image show the artifacts and halos in the resultant image. Multi-scale Laplacian pyramid decomposition of each version of the input image is performed at 5 levels. This means if the image size is 256X256, Laplacian operator is applied on it to obtain the first level of pyramid and then the image is scaled down by 2 for next level and Laplacian operator is applied again to find that level. Image is scaled down and same process is followed till image reaches the size of 16X16. Similarly, Gaussian pyramid of normalized weight map is found out by convolving with Gaussian kernel at the same number of levels as Laplacian pyramid. Now, the corresponding levels of each version are fused to form the fused pyramid using Eq. 10.

$$pyramid^l(i, j) = \sum_{k=1}^2 G^l(W_k(i, j)) L^l(I_k(i, j)) \quad (10)$$

where, pyramid^l is the fused pyramid at level l , G^l indicates Gaussian pyramid level l , L^l indicates Laplacian pyramid level l .

The different levels of the fused pyramid are then composed starting from the highest level, i.e., the pyramid layer at level 5 is upscaled by 2 and then added to level 4, then the resultant is upscaled by 2 and added to level 3 and this process continues till level 1 is reached to find the final fused image. This multi-scale Laplacian fusion process is relatively simple and fast. The results tend to be free from artifacts as fusing at multiple scales suppress sharp transitions.

4. Results and Discussion

For establishing the technique, we have compared FUIER with state-of-the-art techniques, i.e., Dehazing by dark channel prior¹⁸, WCID¹¹, Automatic Red Channel (ARC) underwater restoration¹³ and the Ancuti *et al.*¹ technique. FUIER is implemented in MATLAB version 2015a on an Intel i5 2.60 GHz processor.

4.1. Datasets and Performance Metrics

FUIER has been tested on different images taken from the internet, images from the Ancuti *et al.* CVPR paper² and underwater images from SUN database⁴⁰. It has been tested on more than 200 images for performance evaluation. Recently, a few underwater image databases have been developed namely TURBID dataset¹² and WHOI color correction dataset³². The pictures of TURBID dataset are generated by experimentation for simulation of images in the turbid water body and WHOI (Woods Hole Oceanographic Institution) color correction dataset have original images along with reference images generated by the color correction method developed by scientists of WHOI. Thus, a comparison can be done with the results given on WHOI website³² using reference based performance measures like PSNR (Peak Signal to Noise Ratio) and MSE (Mean Squared Error) but these reference based performance measures cannot be used for quantitative evaluation of other underwater images. Other than these datasets, underwater images neither have any database with ground truth values nor any universally accepted quantitative measure for evaluating the extent of image enhancement. Thus, assessing the performance of underwater image enhancement methods is very challenging.

There are few non-reference based quantitative performance measures which have been used to evaluate the quality of the results namely, Entropy¹⁶, Δ (Difference)²⁵, HS (Histogram Spread)³⁵, UIQM (Underwater Image Quality measure)²⁸ and UCIQE (Underwater Color Image Quality Measure)⁴³. Entropy is general performance metric which indicates the information content of the image. The entropy of an image should increase with improvement in image quality. Δ indicates how closely the image follows gray world assumption⁶. Gray world assumption states that the average of the three color channels should be a gray value. Value of Δ should be zero for an image following the gray world assumption. Histogram spread measures the contrast of an image. If the value of histogram spread is 0.5, then the image is considered to have uniform contrast. UIQM and UCIQE are the two performance measures specifically for underwater images. UIQM is combination of color, contrast and sharpness measure which contribute to overall quality of an underwater image. UCIQE quantifies the extent to which contrast and blurriness of an image is reduced. Values of both UIQM and UCIQE increase as image quality enhances.

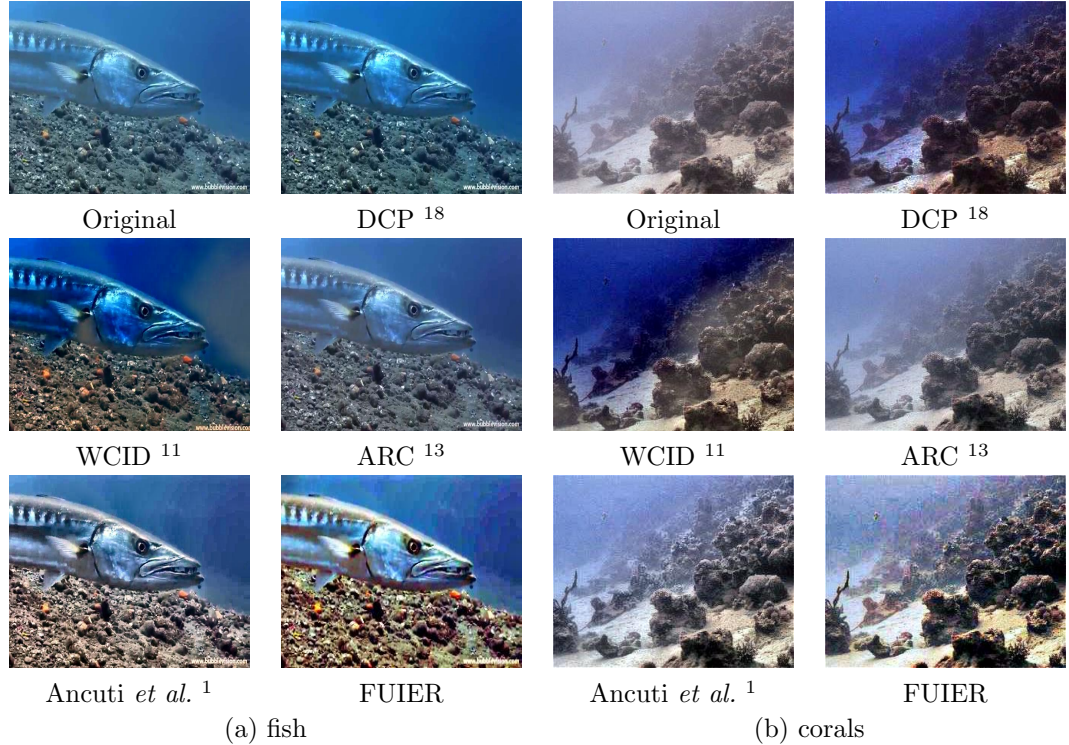


Fig. 5: Results of fish and corals image using state-of-the-art techniques and FUIER. For each type of image, images are in this order: first row: original image, results using DCP, second row: results using WCID and ARC and third row: results using the Ancuti *et al.* technique and FUIER

4.2. Qualitative and Quantitative evaluation of FUIER

For qualitative evaluation of FUIER, few underwater images are shown along with their results obtained using the techniques stated earlier for comparison in Fig. 5-7. Table 1 lists the values of these performance measures for the images shown in Fig. 5-8, for comparison of all the mentioned techniques. For quantitative evaluation, Table 2 lists the average value of mentioned non-reference based performance metrics and average execution time for 200 images tested for evaluation of FUIER and other state-of-the-art-techniques. Bold values in each column of both the tables indicate the best value of that particular metric for an image and underlined value indicates the second best value for that image.

From the visual appearance of images shown in Fig. 5 - 7, it can be seen that DCP ¹⁸ does not bring any noticeable change in the image as it tries to remove the haze only. WCID ¹¹ is removing haze as well as trying to improve the contrast and color of the image but is degrading the overall quality by introducing artifacts in some images, e.g. red color artifact in diver image, green color artifact in diver with rocks image and creation of uneven darker and lighter regions in sea walker image. ARC ¹³, the Ancuti *et al.* ¹ technique and FUIER gives visually good results but on the comparison of the images, it can be seen that details are much better in case of latter than both the former techniques for almost

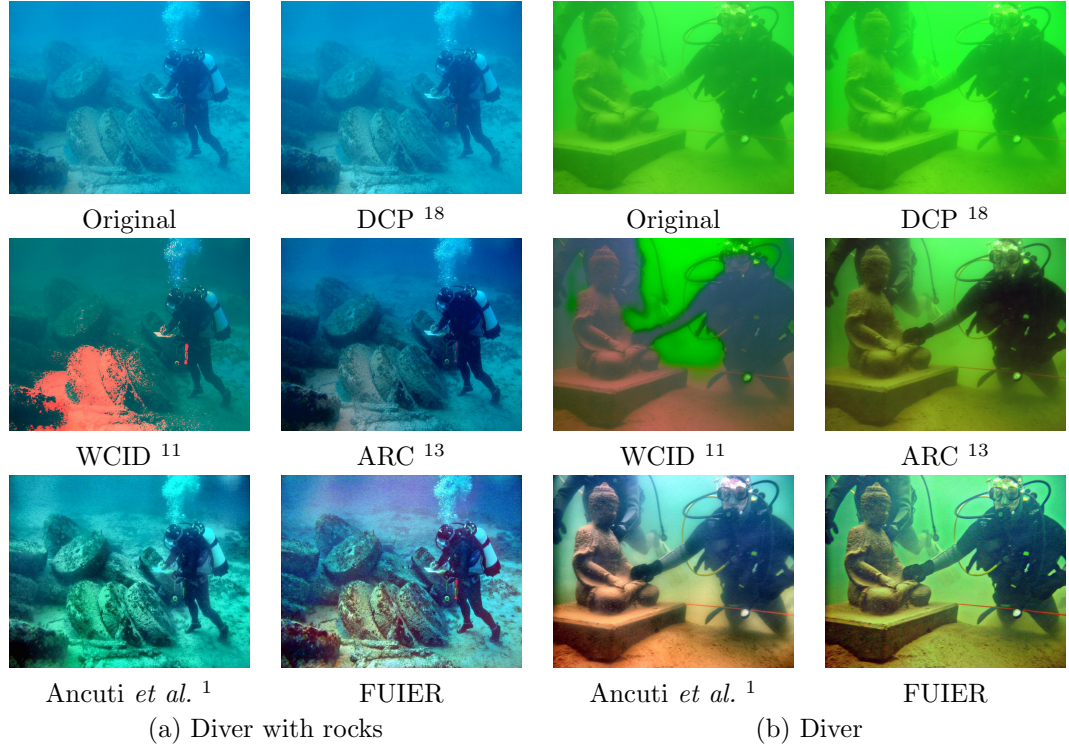
12 *Rajni Sethi, S.Indu*

Fig. 6: Results of diver and diver with rocks image using the state-of-the-art techniques and FUIER. For each type of image, images are in this order : first row: original image, results using DCP, second row: results using WCID and ARC and third row: results using Ancuti *et al.* technique and FUIER

all images, for example, in fishes image, corals in the background are clearly visible as compared to any other results. The Ancuti *et al.* technique is giving better image quality for diver image as this technique is specifically designed for Malaysian water in which diver image is captured.

Following conclusions can be drawn from value of Table 2 and Table 1 for different performance metrics:

Entropy¹⁶: FUIER is performing best in terms of entropy for all the images which means it is enhancing information content of the image better than other techniques which can be seen in the results, For example, In Fig. 5(a), details of fish and terrain below it are clearer in the FUIER fish image than in the results of other techniques and in Fig. 5(b) image, details of the corals in result of the FUIER are better than in other results. DCP and WCID, on the other hand, sometimes reducing the entropy values of a few images, For example, Diver with rocks (Fig. 6(a)) and sea walker image (Fig. 7(a)). ARC is enhancing the information content but not as much as Ancuti *et al.* technique and FUIER. The Ancuti *et al.* technique is giving second best entropy values for most of the images.

Difference (Δ)²⁵: FUIER has the best values for this performance metric for almost all the images which mean there is a balance of colors, i.e., three color channels are averaging

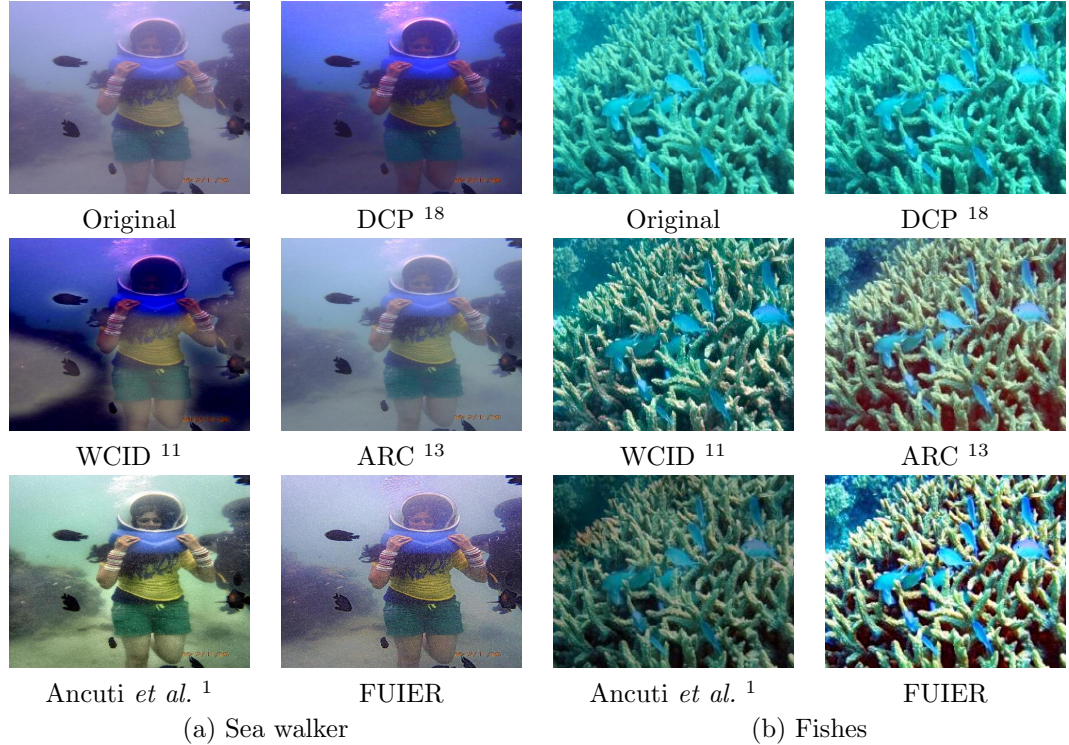


Fig. 7: Results of sea walker and fishes image using state-of-the-art techniques and FUIER. For each type of image, images are in this order : first row: original image, results using DCP, second row: results using WCID and ARC and third row: results using the Ancuti *et al.* technique and FUIER

to a same gray value. The Ancuti *et al.* technique and ARC are also performing well in terms of this performance measure. DCP and WCID, however, are creating a imbalance in colors by increasing the value of this performance metric for some images. For instance, in Fig. 6(a), WCID has introduced false colors and in Fig. 5(b), DCP and WCID image has increased the blue color in the background.

Histogram Spread (HS)³⁵: Histogram spread indicates the contrast performance of an image, i.e., if histogram spreads over the whole dynamic range uniformly. FUIER gives the best results for almost all images for this performance measure also. It can be proven from the visual results also that FUIER gives results with improved contrast. The Ancuti *et al.* technique performs well in terms of contrast but not better than FUIER, e.g., the result of Fig. 5(a) using the Ancuti *et al.* technique has poor contrast as compared to the result of FUIER. However, DCP, WCID and ARC lag in terms of contrast for most of the images which can be seen from the results also as the contrast of the images are not improving to a great extent.

Table 1: Value of non-reference based performance metric for the images shown in Fig. 5 - 7

Metric	Technique	Fish	Corals	Diver	Diver with rocks	Sea Walker	Fishes
Entropy ¹⁶	Original	7.303	7.347	6.711	6.634	7.184	7.481
	DCP ¹⁸	7.475	7.660	6.636	6.625	6.897	7.344
	WCID ¹¹	7.483	7.368	7.050	6.488	7.522	7.569
	ARC ¹³	7.304	7.521	7.696	7.265	7.249	7.549
	Ancuti ¹	<u>7.687</u>	<u>7.786</u>	7.679	<u>7.267</u>	<u>7.717</u>	<u>7.621</u>
	FUIER	7.730	7.920	7.745	7.584	7.783	7.848
Δ^{25}	Original	41.99	14.78	97.80	103.34	45.84	80.86
	DCP ¹⁸	51.47	31.56	108.05	103.36	25.23	87.89
	WCID ¹¹	33.51	26.22	31.93	148.44	35.05	44.04
	ARC ¹³	31.01	<u>18.65</u>	40.67	<u>68.73</u>	22.88	11.45
	Ancuti ¹	<u>19.95</u>	19.32	9.06	84.19	<u>14.42</u>	20.95
	FUIER	19.06	10.31	<u>31.18</u>	44.01	14.02	<u>20.72</u>
HS* ³⁵	Original	0.1680	0.2500	0.1554	0.1180	0.2333	0.3106
	DCP ¹⁸	0.1908	0.2286	0.1558	0.1317	0.2780	0.3232
	WCID ¹¹	0.2118	0.2461	0.2434	0.0777	0.2731	0.2921
	ARC ¹³	0.1725	0.2431	0.1880	0.1664	0.2397	0.3500
	Ancuti ¹	<u>0.2967</u>	<u>0.3072</u>	0.3725	<u>0.2726</u>	0.3673	0.3356
	FUIER	0.3464	0.4052	<u>0.3548</u>	0.3020	<u>0.3373</u>	0.4747
UIQM ²⁸	Original	3.362	4.538	3.559	1.512	3.491	1.455
	DCP ¹⁸	3.462	5.268	3.559	1.342	4.059	0.646
	WCID ¹¹	4.312	4.485	3.575	1.716	4.025	3.084
	ARC ¹³	3.512	4.693	4.205	2.385	3.537	5.034
	Ancuti ¹	3.812	<u>5.029</u>	4.833	<u>3.287</u>	<u>4.712</u>	<u>4.129</u>
	FUIER	<u>3.901</u>	4.717	<u>4.820</u>	4.566	4.887	3.761
UCIQE ⁴³	Original	5.189	7.367	1.466	2.929	3.257	7.380
	DCP ¹⁸	7.595	<u>11.298</u>	1.264	2.766	<u>5.388</u>	6.958
	WCID ¹¹	12.306	10.471	5.647	6.007	5.845	8.408
	ARC ¹³	5.635	7.142	3.660	5.020	3.597	<u>10.765</u>
	Ancuti ¹	7.486	9.732	10.237	<u>5.716</u>	5.195	3.290
	FUIER	<u>9.482</u>	11.310	<u>9.421</u>	4.623	3.938	13.621

*HS stands for Histogram Spread

UIQM²⁸: FUIER always gives results with increased UIQM value. For some images, it gives the best values. From the results, it can be seen that FUIER increases the overall quality of the image by improving the color, contrast and sharpness of the image. DCP is

able to improve only the sharpness of the image. WCID, on the other hand, improves the color, contrast and sharpness for few images for example, images shown in Fig. 5(a), 5(b) and 7(b), but it distorts the colors of few images like those shown in Fig. 6(a), 6(b) and 7(a). Contrast and sharpness of ARC images, except for the image shown in Fig. 5(a) are not better than the results of the Ancuti *et al.* technique and FUIER, resulting in lower UIQM values than the latter two. In terms of average UIQM values, the Ancuti *et al.* technique is giving the best and FUIER is giving the second best results, but from visual results, it can be seen that sharpness and brightness of results of FUIER are better than the results of the Ancuti *et al.* technique.

UCIQE⁴³: From Table 2, it can be seen that FUIER again performs better than all the other techniques. WCID is performing well in terms of this performance metric as it removes the blur effectively but lags in terms of other performance measures leading to poor visual results. ARC and the Ancuti *et al.* technique also perform well, but it can be seen from the visual results as well as the overall values of quantitative measures that FUIER delivers visually appealing results as compared to other techniques.

Execution Time: From Table 2, it is clear that average execution time is in the following increasing order, DCP, ARC, FUIER, Ancuti *et al.* technique, WCID. Thus, DCP takes the least time but it is not suitable for underwater images. WCID does not produce good results and has the highest average execution time. Out of ARC, FUIER and Ancuti *et al.* technique, ARC is the best in terms of execution time but does not produce very good quality images as discussed earlier. There is very little difference in the average execution time of ARC and FUIER. Thus, we can say that FUIER gives good quality results with lesser time complexity as compared to all other state-of-the-art techniques.

Table 2: Average Value of performance metrics and execution time for 200 underwater images for comparison of FUIER and state-of-the-art techniques

Technique	Entropy ¹⁶	Δ ²⁵	HS ³⁵	UIQM ²⁸	UCIQE ⁴³	Time (in sec)
Original	6.970	47.04	0.1867	3.750	4.059	-
DCP ¹⁸	6.928	50.46	0.1844	3.750	4.954	0.078
WCID ¹¹	6.965	43.05	0.2183	3.760	7.199	4.19
ARC ¹³	6.994	24.63	0.1996	4.3228	5.885	<u>0.94</u>
Ancuti ¹	<u>7.671</u>	<u>19.34</u>	<u>0.3240</u>	4.690	<u>7.441</u>	1.89
FUIER	7.774	16.90	0.3552	4.648	7.923	1.07

As mentioned earlier, there are two datasets for underwater images i.e. WHOI dataset³² and TURBID dataset¹², so for further comparison of FUIER with state-of-the-art methods, we have shown a few images from these databases in Fig. 8. Table 3 gives the value of reference based PSNR(Peak Signal to Noise Ratio) and MSE(Mean Squared Error) along with the non-reference based performance metric values for these images. PSNR should be higher and MSE should be lower for a better image.

From the table values, it can be seen that FUIER has the best PSNR and MSE values among all techniques. Visual results of FUIER and the Ancuti *et al.* technique have better information content and are more appealing as compared to other techniques which is also proven by the performance measure values. However, the Ancuti *et al.* technique is not performing consistently for every type of image. It is not improving contrast of few images

(e.g., fishes image., Fig.7(b)) and not able to remove haze properly for few other images (e.g., corals image, Fig.5(b)). From quantitative and qualitative analysis, we can say that FUIER performs well for underwater images captured in different conditions (turbidity, depth, salinity etc.) using computationally less intensive approach, as proven by the average execution time.

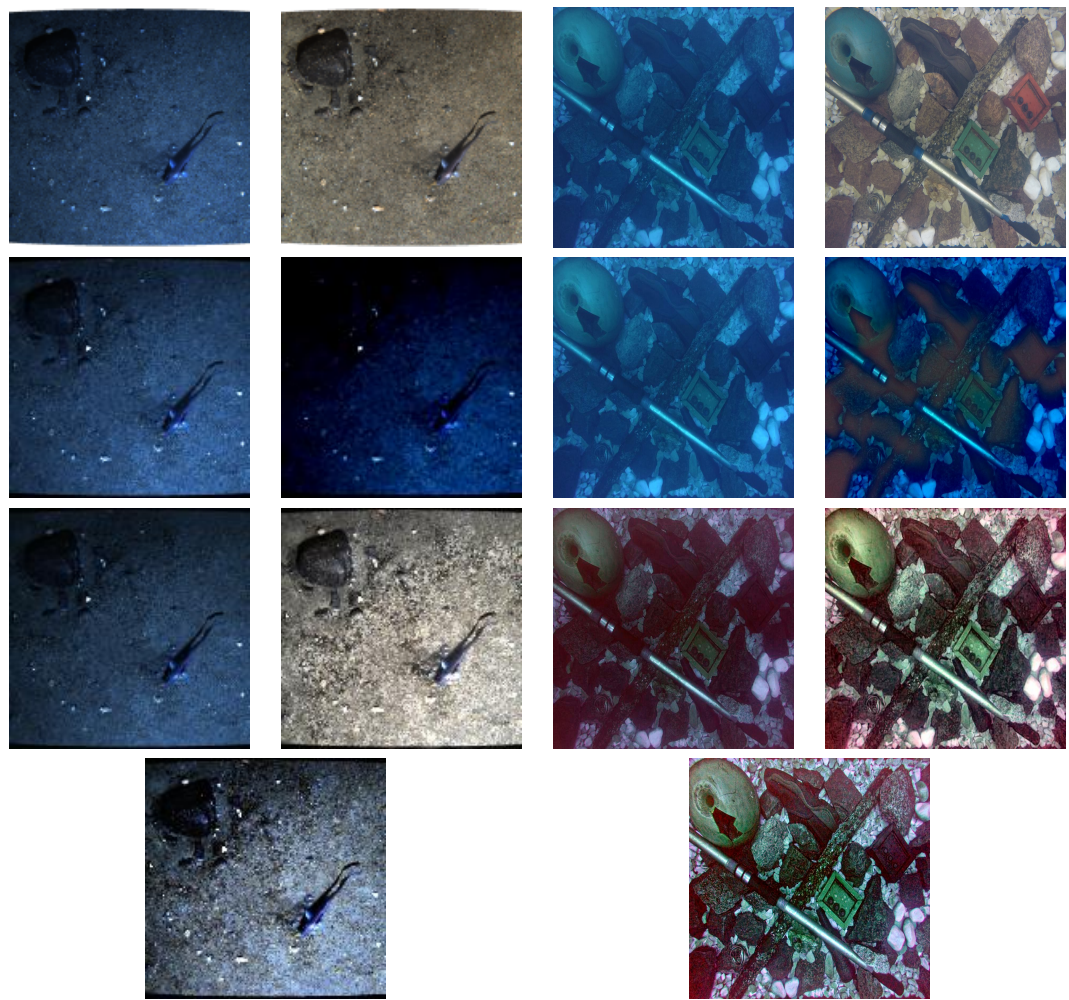


Fig. 8: Results of image 1 and image 2 using the state-of-the-art techniques and FUIER. For each type of image, images are in this order : first row: original image, results using DCP, second row: results using WCID and ARC and third row: results using Ancuti *et al.* technique and FUIER

Table 3: Value of reference based performance metrics for images shown in Fig. 8

Image	Technique	PSNR	MSE	Entropy	Δ	HS	UIQM	UCIQE
Image1	Original	-	-	5.911	26.68	0.1244	3.383	0.352
	Reference	-	-	6.798	8.943	0.1404	4.971	1.009
	DCP ¹⁸	14.42	2349.6	7.295	30.69	0.1493	4.4018	1.179
	WCID ¹¹	10.62	6129.1	6.852	27.89	0.1242	2.176	3.438
	ARC ¹³	13.85	2676.4	7.034	20.93	0.1423	4.388	0.831
	Ancuti ¹	13.92	2635.3	7.780	5.57	0.3124	5.372	2.516
Image2	FUIER	16.48	1461.6	7.809	14.59	0.3360	4.655	1.211
	Original	-	-	5.157	52.12	0.1832	2.786	0.6711
	Reference	-	-	6.807	3.29	0.2066	4.430	4.056
	DCP ¹⁸	12.89	3339.3	6.678	55.60	0.1775	4.270	3.207
	WCID ¹¹	10.52	5772	6.762	42.09	0.1528	4.171	7.216
	ARC ¹³	13.24	3080.8	6.610	12.52	0.1632	4.984	3.522
Image3	Ancuti ¹	15.53	1820	7.670	6.36	0.3320	5.143	7.480
	FUIER	15.76	1724.3	7.689	4.51	0.3216	5.020	9.803

For a more exhaustive comparison, comparative analysis has been done with a CNN based technique ³⁷. A few images along with the results have been taken from the article ³⁷ and are shown along with the results of FUIER in Fig. 9. The values of various performance metrics of the images are depicted in table 4.

It is clear from the images shown in Fig. 9 that the CNN based technique ³⁷ produces good results but the contrast is poor whereas FUIER produces better images with more clarity.

Table 4: Value of performance metrics for images shown in Fig. 9

Image	Technique	Entropy	Δ	HS	UIQM	UCIQE
Rocks	Original	3.73	10.35	0.0365	4.56	1.49
	CNN based ³⁷	6.14	4.23	0.1232	5.08	0.79
	FUIER	7.12	5.72	0.2615	5.04	4.43
Medium	Original	4.93	15.00	0.093	4.95	0.27
	CNN based ³⁷	6.37	1.50	0.1475	5.28	0.33
	FUIER	7.44	4.05	0.3211	5.86	1.78
Shallow	Original	4.30	10.13	0.1455	2.70	1.01
	CNN based ³⁷	5.56	1.24	0.1589	3.39	0.48
	FUIER	7.73	2.19	0.3699	4.66	5.71

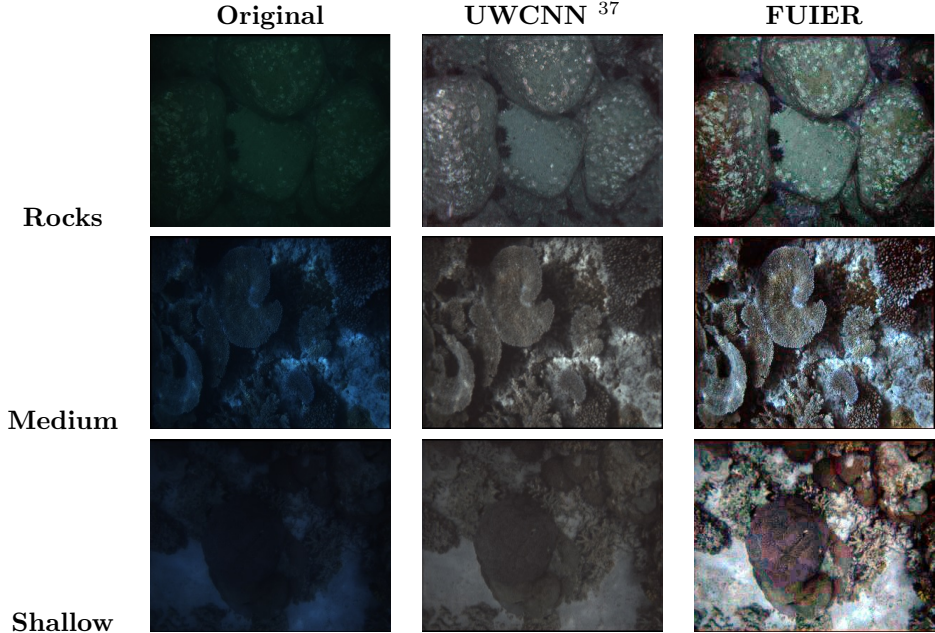


Fig. 9: Results of images taken from ³⁷ and results using FUIER.

In terms of quantitative measures, Entropy, HS and UCIQE values of FUIER are always better than for the CNN based technique ³⁷. This means information content, contrast and blurriness of the image are improved better in images obtained using FUIER. UIQM values of the CNN based technique ³⁷ are better for a few images but again FUIER outperforms it for most of the images. Both the CNN based technique ³⁷ and FUIER lower the Δ values close to zero but gray world assumption is being followed more closely by the results of the former. CNN based technique ³⁷ has tested various types of underwater images (sands, rocks, kelp ³⁷) taken at different depths (shallow, medium and deep corals ³⁷). FUIER gives good results for all of them. CNN requires training for adjusting the parameters of image restoration techniques whereas FUIER requires no parameter adjustment or training. Therefore, FUIER is suitable for all types of underwater images.

4.3. Applications

FUIER finds its applicability in the following computer vision related fields:

Local Feature Matching: One of the basic tasks of computer vision algorithms is local feature points matching, which forms the basis for underwater studies like classification of marine animals, fish species recognition etc.

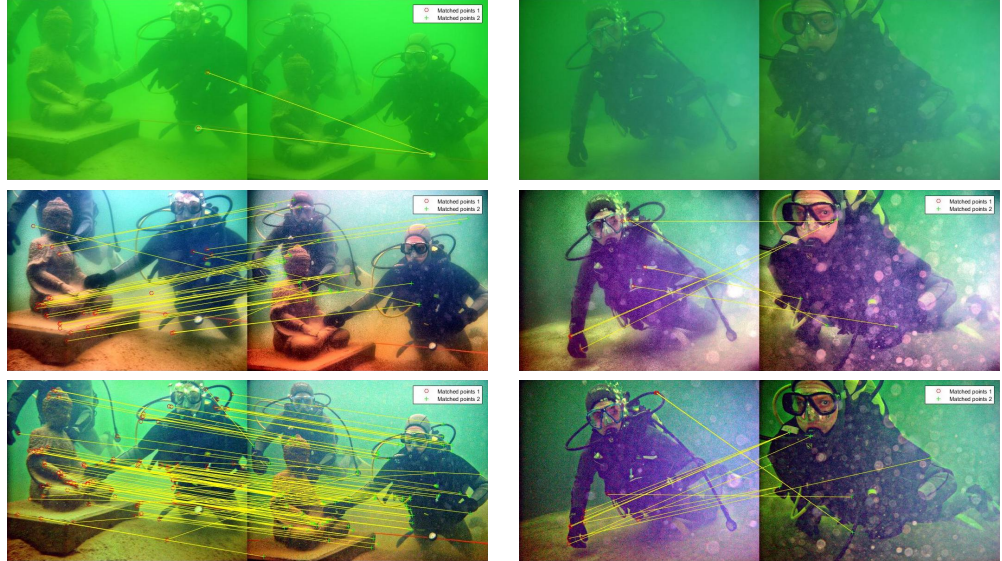


Fig. 10: First row contains the original pair of images with only 2 SURF features matching in the first column and none in the second column, second row contains the enhanced pair of images using the Ancuti *et al.* technique with 37 SURF features matching in the first column and 7 features in the second column and third row contains the enhanced pair of images using FUIER with 104 SURF features matching in the first column and 13 matching in the second column.

Local features are indifferent to rotation, scaling and motion changes. We have employed SURF⁴ operator to compute and match feature blobs for a pair of underwater images and repeated the same process for the enhanced versions of the corresponding pair of images. We used the SURF feature matching provided by MATLAB. We enhanced the pair of images using the Ancuti *et al.*¹ technique results and FUIER. The results are very promising which shows that the number of local feature points increase significantly by FUIER as compared to Ancuti *et al.*¹ and are shown in Fig. 10.

Edge Detection: Edge detection is an important processing task in image processing which further assists in various fields of computer vision related to underwater studies like segmentation in order to localize coral reefs. We have employed Laplacian of Gaussian (LoG)²² to find the edges in the images. Edge detection results of the original image and enhanced images using Ancuti *et al.* technique and FUIER are shown in Fig. 11.

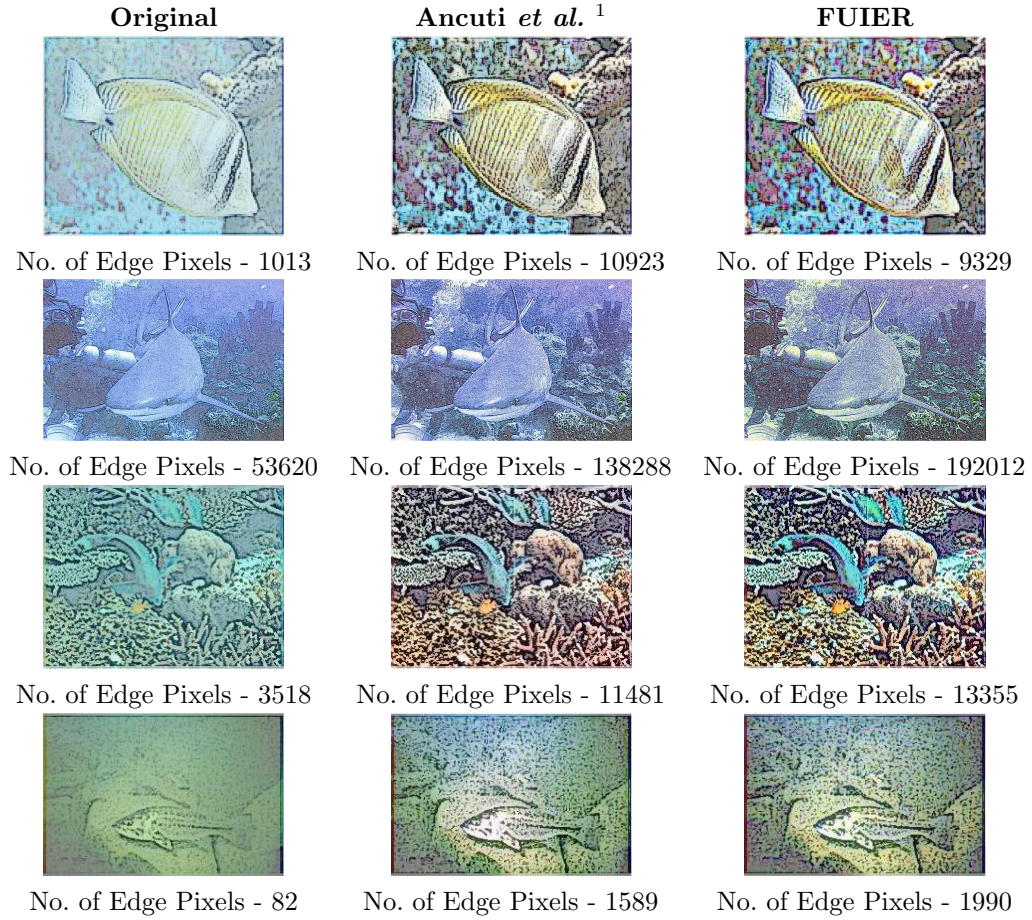


Fig. 11: First column: original images second column: the Ancuti *et al.* technique images and third column: FUIER images. Each image is blended with its edge detection result and the number of edge pixels of each image is mentioned below it.

It is clear from these results that both FUIER and the Ancuti *et al.* technique generate enhanced images with more edges as compared to the original image. However, images of FUIER have more edge pixel count than the Ancuti *et al.* technique¹ for most of the images.

5. Conclusions

In this paper, a fusion of underwater image enhancement and restoration has been presented. FUIER is a simple yet powerful method for improving the visual quality of every type of underwater image. Simple and basic techniques like HE, contrast stretching and DCP have been employed but with effective and meaningful weight maps so that the required features are taken and fused to derive resultant image. The resultant image has

improved color, contrast and visibility. The advantage of FUIER is that it incorporates color correction, contrast correction and blurring into two versions and takes essential features based on weights so as to generate an enhanced output image. All the major issues in underwater images have been handled using simple and computationally less intensive techniques employed in FUIER. The results of FUIER are visually appealing and better as compared to state-of-the-art techniques and are easily applicable in many computer vision algorithms. However, FUIER lags, in terms of color reproduction when there is deep haze in the underwater images. The future scope may include an attempt to tackle this problem.

References

1. C. O. Ancuti, C. Ancuti, C. D. Vleeschouwer and P. Bekaert, Color balance and fusion for underwater image enhancement, *IEEE Transactions on Image Processing* **27** (Jan 2018) 379–393.
2. C. Ancuti, C. O. Ancuti, T. Haber and P. Bekaert, Enhancing underwater images and videos by fusion, in *Computer Vision and Pattern Recognition (CVPR), 2012 IEEE Conference on* (2012) pp. 81–88.
3. S. Anwar, C. Li and F. Porikli, Deep underwater image enhancement, *arXiv preprint arXiv:1807.03528* (2018).
4. H. Bay, T. Tuytelaars and L. Van Gool, Surf: Speeded up robust features, in A. Leonardis, H. Bischof and A. Pinz (eds.), *Computer Vision – ECCV 2006* (Springer Berlin Heidelberg, Berlin, Heidelberg, 2006) pp. 404–417.
5. S. Bazeille, I. Quidu, L. Jaulin and J. P. Malkasse, Automatic underwater image pre-processing, *Proceedings of 1900*(1) (2006) p. 8.
6. G. Buchsbaum, A spatial processor model for object colour perception, *Journal of the Franklin Institute* **310**(1) (1980) 1 – 26.
7. P. J. Burt and E. H. Adelson, The laplacian pyramid as a compact image code, in *Readings in Computer Vision* (Elsevier, 1987) pp. 671–679.
8. N. Carlevaris-Bianco, A. Mohan and R. M. Eustice, Initial results in underwater single image dehazing, *MTS/IEEE Seattle, OCEANS 2010* (2010).
9. A. T. Çelebi and S. Ertürk, Visual enhancement of underwater images using empirical mode decomposition, *Expert Systems with Applications* **39**(1) (2012) 800–805.
10. L. Chao and M. Wang, Removal of water scattering, *ICCET 2010 - 2010 International Conference on Computer Engineering and Technology, Proceedings* **2** (2010) 35–39.
11. J. Y. Chiang and Y. C. Chen, Underwater image enhancement by wavelength compensation and dehazing, *IEEE Transactions on Image Processing* **21**(4) (2012) 1756–1769.
12. A. Duarte, F. Codevilla, J. D. O. Gaya and S. S. C. Botelho, A dataset to evaluate underwater image restoration methods, in *OCEANS 2016 - Shanghai* (April 2016) pp. 1–6.
13. A. Galdran, D. Pardo, A. Picón and A. Alvarez-Gila, Automatic Red-Channel underwater image restoration, *Journal of Visual Communication and Image Representation* **26** (2015) 132–145.
14. C. Gao, J. Zhou, C. Liu and Q. Pu, Image enhancement based on fractional directional derivative, *International Journal of Machine Learning and Cybernetics* **6**(1) (2015) 35–41.
15. Y. Gao, H. Li and S. Wen, Restoration and Enhancement of Underwater Images Based on Bright Channel Prior, *Mathematical Problems in Engineering* **2016** (2016).
16. R. C. Gonzalez, R. E. Woods *et al.*, Digital image processing (1992).
17. K. He, J. Sun and X. Tang, Guided image filtering, *IEEE Transactions on Pattern Analysis and Machine Intelligence* **35** (June 2013) 1397–1409.

22 *Rajni Sethi, S.Indu*

18. K. He, J. Sun and X. Tang, Single image haze removal using dark channel prior, *IEEE transactions on pattern analysis and machine intelligence* **33**(12) (2011) 2341–2353.
19. K. Iqbal, M. Odetayo, A. James, R. A. Salam and A. Z. H. Talib, Enhancing the low quality images using unsupervised colour correction method, *Conference Proceedings - IEEE International Conference on Systems, Man and Cybernetics* (2010) 1703–1709.
20. K. Iqbal, R. A. Salam, A. Osman and A. Z. Talib, Underwater Image Enhancement Using an Integrated Colour Model, *International Journal of Computer Science* **34**(2) (2007) 239—244.
21. J. S. Jaffe, Computer modeling and the design of optimal underwater imaging systems, *Oceanic Engineering, IEEE Journal of* (1990).
22. R. Jain, R. Kasturi and B. G. Schunck, *Machine vision* (McGraw-Hill New York, 1995).
23. L. Jolla, SINGLE UNDERWATER IMAGE ENHANCEMENT USING DEPTH ESTIMATION BASED ON BLURRINESS Yan-Tsung Peng , Xiangyun Zhao and Pamela C . Cosman Department of Electrical and Computer Engineering , University of California , San Diego , , *International Conference on Image Processing (ICIP)* (2015) 2–6.
24. T. Kadir and M. Brady, Saliency, scale and image description, *International Journal of Computer Vision* **45** (Nov 2001) 83–105.
25. N. Kwok, H. Shi, Q. Ha, G. Fang, S. Chen and X. Jia, Simultaneous image color correction and enhancement using particle swarm optimization, *Engineering Applications of Artificial Intelligence* **26**(10) (2013) 2356 – 2371.
26. C. Y. Li, J. C. Guo, R. M. Cong, Y. W. Pang and B. Wang, Underwater image enhancement by Dehazing with minimum information loss and histogram distribution prior, *IEEE Transactions on Image Processing* **25**(12) (2016) 5664–5677.
27. H. Lu, Y. Li and S. Serikawa, Underwater image enhancement using guided trigonometric bilateral filter and fast automatic color correction, *2013 IEEE International Conference on Image Processing, ICIP 2013 - Proceedings* (2013) 3412–3416.
28. K. Panetta, C. Gao and S. Agaian, Human-visual-system-inspired underwater image quality measures, *IEEE Journal of Oceanic Engineering* **41** (July 2016) 541–551.
29. J. Perez, A. C. Attanasio, N. Nechyporenko and P. J. Sanz, A deep learning approach for underwater image enhancement, in *International Work-Conference on the Interplay Between Natural and Artificial Computation* (2017) pp. 183–192.
30. H. Qin, X. Li, J. Liang, Y. Peng and C. Zhang, DeepFish: Accurate underwater live fish recognition with a deep architecture, *Neurocomputing* (2016).
31. R. Schettini and S. Corchs, Underwater image processing: State of the art of restoration and image enhancement methods, *EURASIP Journal on Advances in Signal Processing* **2010** (Apr 2010) p. 746052.
32. H. Singh, WHOI color correction dataset <https://web.whoi.edu/singh/underwater-imaging/datasets/color-correction/>.
33. J. A. Stark, Adaptive image contrast enhancement using generalizations of histogram equalization, *IEEE Transactions on image processing* **9**(5) (2000) 889–896.
34. L. A. Torres-Méndez and G. Dudek, Color correction of underwater images for aquatic robot inspection, in A. Rangarajan, B. Vemuri and A. L. Yuille (eds.), *Energy Minimization Methods in Computer Vision and Pattern Recognition* (Springer Berlin Heidelberg, Berlin, Heidelberg, 2005) pp. 60–73.
35. A. K. Tripathi, S. Mukhopadhyay and A. K. Dhara, Performance metrics for image contrast, in *2011 International Conference on Image Information Processing* (Nov 2011) pp. 1–4.
36. H. Wang, R. Zhao, Y. Cen, L. Liang, Q. He, F. Zhang and M. Zeng, Low-rank matrix

- recovery via smooth rank function and its application in image restoration, *International Journal of Machine Learning and Cybernetics* **9** (Sep 2018) 1565–1576.
37. Y. Wang, J. Zhang, Y. Cao and Z. Wang, A deep cnn method for underwater image enhancement, in *2017 IEEE International Conference on Image Processing (ICIP)* (Sept 2017) pp. 1382–1386.
 38. W. E. Watson, S. R. Benson and J. T. Harvey, An application of underwater imaging for marine vertebrate ecology, in *OCEANS 2010 MTS/IEEE SEATTLE* (Sept 2010) pp. 1–6.
 39. X. Wei, H. Wang, G. Guo and H. Wan, Multiplex image representation for enhanced recognition, *International Journal of Machine Learning and Cybernetics* **9** (Mar 2018) 383–392.
 40. J. Xiao, J. Hays, K. A. Ehinger, A. Oliva and A. Torralba, Sun database: Large-scale scene recognition from abbey to zoo, in *2010 IEEE Computer Society Conference on Computer Vision and Pattern Recognition* (June 2010) pp. 3485–3492.
 41. C. Yan, N. Sang and T. Zhang, Local entropy-based transition region extraction and thresholding, *Pattern Recognition Letters* **24**(16) (2003) 2935–2941.
 42. H. Y. Yang, P. Y. Chen, C. C. Huang, Y. Z. Zhuang and Y. H. Shiau, Low complexity underwater image enhancement based on dark channel prior, *Proceedings - 2011 2nd International Conference on Innovations in Bio-Inspired Computing and Applications, IBICA 2011* (2011) 17–20.
 43. M. Yang and A. Sowmya, An underwater color image quality evaluation metric, *IEEE Transactions on Image Processing* **24** (Dec 2015) 6062–6071.
 44. D. R. Yoerger, A. M. Bradley, B. B. Walden, M. H. Cormier and W. B. F. Ryan, Fine-scale seafloor survey in rugged deep-ocean terrain with an autonomous robot, in *Proceedings 2000 ICRA. Millennium Conference. IEEE International Conference on Robotics and Automation. Symposia Proceedings (Cat. No.00CH37065)*, Vol. 2 (2000) pp. 1787–1792 vol.2.
 45. C. Zhang, X. Zhang and D. Tu, Underwater image enhancement by fusion, in *International Workshop of Advanced Manufacturing and Automation* (2017) pp. 81–92.